Electronic properties of some CaF_2-structure intermetallic compounds

P. M. Th. M. van Attekum, G. K. Wertheim, G. Crecelius,* and J. H. Wernick
Bell Laboratories, Murray Hill, New Jersey 07974
(Received 20 March 1980)

The valence-band structure, plasmon energies, core-electron singularity indices, and charge transfer of some CaF_2-structure intermetallic compounds have been studied. The results are compatible with other available experimental data and with band-structure calculations, and confirm the free-electron character of the valence bands near the Fermi energy. Significant charge transfer in the antifluorite direction was found in all the compounds studied.

INTRODUCTION

The formation of crystallographically ordered intermetallic compounds depends in part on the ratio of atomic sizes which may favor a particular spatial arrangement, and in part on charge transfer which brings Coulomb forces into play.[1] In the case of the CsCl-structure intermetallics, those with smaller charge transfer, e.g., AgCd, are readily disordered by quenching while those with large charge transfer, e.g., AuCs, remain ordered and behave more like ionic insulators.[2] In the CaF_2-structure compounds $AuAl_2$ and Mg_2Sn the atomic sizes of the constituents are quite similar, suggesting that charge transfer must be responsible for the strong tendency to form ordered intermetallic phases.

In the CaF_2 structure, each Ca is surrounded by eight F atoms at the corners of a cube and each F by four Ca atoms at the corners of a regular tetrahedron. Many of the intermediate phases with this structure are metallic in behavior, e.g., $PtSn_2$, $AuGa_2$, $AuAl_2$.

In some of the intermediate phases having this structure the more metallic (electropositive) atom occupies the nonmetallic (electronegative) fluorine sites of the CaF_2 lattice. These compounds are occasionally referred to as having the antifluorite structure because they are "anti-isomorphous" with CaF_2. The list of anti-isomorphous compounds contains insulators, e.g., Na_2O, intrinsic semiconductors, e.g., Mg_2Si, and metals, e.g., Mg_2Pb. For the anti-isomorphous compounds, the physical properties are increasingly metallic with increasing molecular weight. Evidence for the dominance of covalent bonding in Mg_2Sn is obtained from the fact that the conductivity of molten Mg_2Sn is about the same as that of molten Sn.[3]

We have investigated several of these compounds using x-ray photoelectron spectroscopy (XPS) in order to elucidate their electronic structure. Valence-band spectra obtained by this technique provide a representation of the occupied density of states in which the electronic states are weighted by their photoelectric cross section. Such data may be used to test band-structure calculations. The shift of core-electron binding energies has a component which reflects the charge transfer. Less well recognized is the fact that core-electron spectra also contain information relevant to the nature of the outer electronic orbitals in the plasmon-loss structure[4,5] and the line shape.[6-8]

The excitation of a plasmon produces a subsidiary line on the high binding-energy side of a core photoemission line. In practice multiple plasmon losses, as well as distinct bulk- and surface-plasmon losses can be identified. The plasmon energy, the separation between the main XPS line and the satellite, is given by

$$\hbar\omega_p = \hbar(4\pi ne^2/m)^{1/2}, \tag{1}$$

where n is the valence-electron density and m is the electron mass. In free-electron metals, well-defined plasmon losses are observed. In metals which deviate strongly from free-electron behavior, as do the noble metals, the loss structure becomes broad and weak and is often dominated by interband transitions.

The many-body screening response of the conduction electrons, sometimes called the MND effect,[6,7] manifests itself in the shape of the core-electron XPS lines.[8] It is brought about by an integrable infinity of small excitations as the conduction electrons react to screen the core hole. The result is a characteristic one-sided, long-tailed, power-law line shape of the form

$$I(\varepsilon) = (\xi/\varepsilon)^{1-\alpha}, \tag{2}$$

where ε is the energy of the excitations and ξ is a bandwidth. The singularity index, α, is defined in terms of the Friedel phase shifts, δ_l, by

$$\alpha = \sum_{l=0}^{\infty} 2(2l+1)\left(\frac{\delta_l}{\pi}\right)^2 . \quad (3)$$

Convolution with the hole-state lifetime Lorentzian yields[8]

$$I(\varepsilon) = \frac{\cos[\pi\alpha/2 + (1-\alpha)\arctan(\varepsilon/\gamma)]}{(\varepsilon^2+\gamma^2)^{(1-\alpha)/2}}, \quad (4)$$

where γ is the half-width at half maximum of the Lorentzian. For free-electron metals with only s, p, and d character at the Fermi energy, α is restricted to in the interval

$$\tfrac{1}{18} \le \alpha \le \tfrac{1}{2} . \quad (5)$$

The MND effect has been studied in detail in the simple metals Li, Na, Mg, and Al.[9]

In addition to these electronic excitations, there is also the possibility of a Franck-Condon excitation of the lattice by Coulomb forces between the photoionized atom and its neighbor. This manifests itself as a Gaussian broadening of the spectrum, and is most important in insulators.

SAMPLE PREPARATION

The Mg compounds were prepared by melting stoichiometric components in graphite boats. The Au compounds were prepared by induction-melting stoichiometric quantities of constituents under an argon atmosphere in recrystallized Al_2O_3 crucibles. This was followed by zone melting (six passes) in recrystallized Al_2O_3 boats. High-resistance ratios can be obtained by zero-refining $AuGa_2$, $AuIn_2$, and $AuAl_2$, suggesting that they are stoichiometric well-ordered line phases in the respective phase diagrams. Moreover, Wernick[10] has shown that although the atomic sizes of Au and Pt and the lattice constants of $AuGa_2$ and $PtGa_2$ are favorable for extensive solid solubility, little mutual solid solubility does occur, suggesting that the electron concentration in these compounds cannot be altered.

Clean surfaces for the XPS experiments were obtained by filing or scraping the samples in a 10^{-7} Pa vacuum in a preparation chamber attached to a Hewlett-Packard 5950A ESCA (electron spectroscopy for chemical analysis) spectrometer.

VALENCE-BAND SPECTRA

The XPS valence-band spectra of Mg_2Sn and Mg_2Pb, Fig. 1, give a good representation of the actual density of states because the Mg 3s and Sn 5s5p (or Pb 6s6p) cross sections are comparable.[11] The lower broad peak near 8 eV consists predominantly of Sn (or Pb) s orbitals, the broader structure closer to E_F contains Sn (or Pb) p-orbital contributions. The s and p bands of Sn and Pb

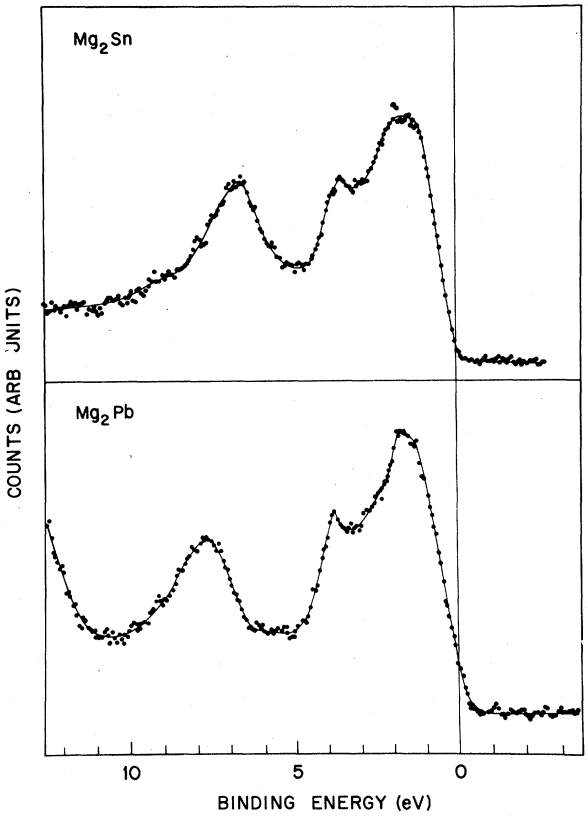

FIG. 1. Valence-band spectra of Mg_2Sn and Mg_2Pb.

are somewhat narrower than in the elemental metals. This reflects the reduction of the bandwidth by the increase in the distance between like atoms compared to that in the pure metals.

The valence-band spectra of these compounds are in agreement with earlier work[12] as well as with the corresponding band-structure calculations.[12-14] The latter suggest that the bands at the top of the valence band in both Mg_2Sn and Mg_2Pb are free-electron-like. Tejeda *et al.*[12] studied Mg_2X (X=Si, Ge, and Sn) with XPS. Our valence-band spectrum of Mg_2Sn (Fig. 1) is similar to theirs. (Here the resolution is slightly better and spurious effects due to x-ray satellites are absent.) The valence-band spectrum of Mg_2Pb is very similar to that of Mg_2Sn (Fig. 1). This is in good agreement with the calculated band profiles for Mg_2Sn (Ref. 13) and Mg_2Pb (Ref. 14) which show almost identical band shapes. The major difference lies in the energy separation between the top of the valence band at Γ_{15} and the bottom of the conduction band at X_1 which decreases from about 0.3 eV in Mg_2Sn to an overlap of about 0.01 eV in Mg_2Pb. The latter point is nicely confirmed by the location of the Fermi energy in Fig. 1 which shows that Mg_2Pb is a metal, while Mg_2Sn is a

small band-gap semiconductor.[15,16]

The valence-band spectra of the AuX_2 compounds (X=Al, Ga, In), Fig. 2, are dominated by the Au $5d$ contribution which has a cross section 10 to 20 times that of the conduction electrons of the Au or X atom.[11] The narrowing of the $5d$ band relative to that of pure gold is apparent. In these compounds, the Au-Au distance is ~1.5 times that in Au metal. The shift to greater binding energy of the Au $5d$ bands is largely attributable to the reduced s-d hybridization which makes the Au atoms more nearly $5d^{10}$ in the AuX_2 compounds. The conduction-band part of the spectra contains contributions from sp electrons of the X atoms and the $6s$ electrons of the Au atoms. The cross sections of the X atom sp electrons are two or three times those of the Au $6s$ electrons.[11]

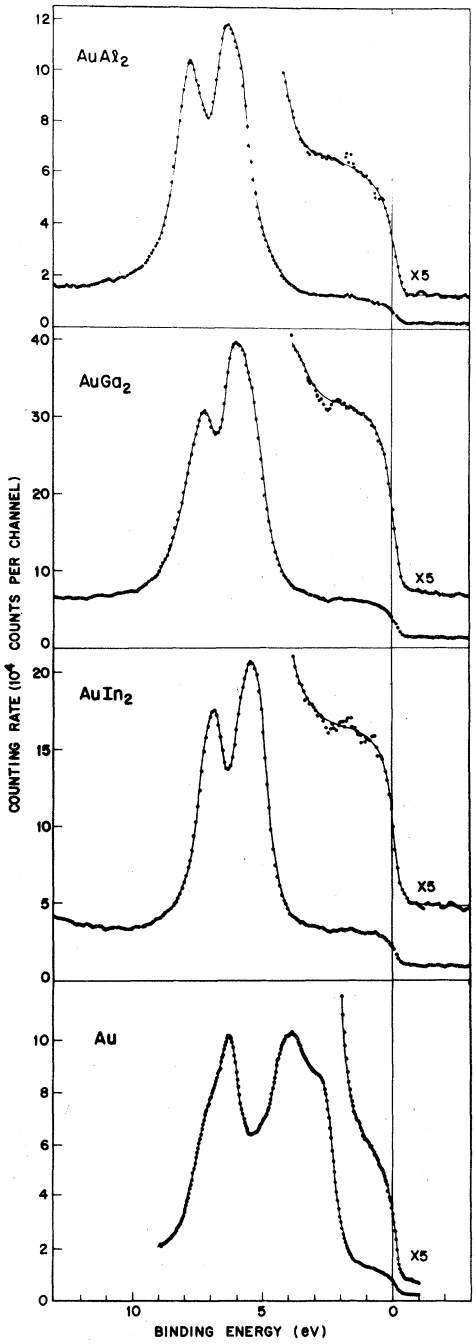

FIG. 2. Valence-band spectra of AuX_2 (X= Al, Ga, In) compared with that of Au metal.

The experimental valence bands shown in Fig. 2 are in good agreement with band-structure calculations.[17] According to the calculation for $AuAl_2$, $AuGa_2$, and $AuIn_2$, the bands near the Fermi energy are free-electron-like with mainly Al, Ga, or In s and p character and small admixture of Au $6s$-band character.[17] The Au $5d$ bands lie further below E_F than in Au metal and are greatly narrowed.[16] As a consequence, the density of states at the Fermi energy has no contribution from Au $5d$ states.

These conclusions are also supported by deHaas-van-Alphen-effect results[18] for $AuAl_2$, $AuGa_2$, and $AuIn_2$ which are in fairly good agreement with a Fermi surface based on a nearly-free-electron model, as are magnetoresistance studies[19] of $AuAl_2$.

PLASMON LOSSES

The plasmon energies and line shapes were determined using methods previously described.[20] The experimental plasmon-loss spectrum is calculated as the convolution of the experimental no-loss line with a plasmon-loss energy-distribution spectrum represented by asymmetric Lorentzians. The same plasmon-loss energy-distribution functions are used for all core electrons. Figure 3 illustrates the removal of the plasmon losses from an experimental spectrum. A bulk- and a surface-plasmon loss as well as multiple combinations of plasmons were taken out. In Table I we list the bulk-plasmon energies ($\hbar\omega_b$) determined by this subtraction process. The corresponding surface-plasmon energies were taken to be $\hbar\omega_b/\sqrt{2}$ as expected for a vacuum interface.

Figure 4 illustrates the importance of the removal of the plasmon losses from an experimental spectrum. Without the correction for the Sn $4d$ plasmon losses, an analysis of the line shape of the Mg $2p$ line in Mg_2Sn is virtually precluded.

It is remarkable that clear plasmon-loss satellites are observed in all of these intermetallics, even those containing Au and Pt, which as pure metals show almost no plasmon structure. It is an interesting observation that for Mg_2Sn and Mg_2Pb the experimental plasmon energy is equal

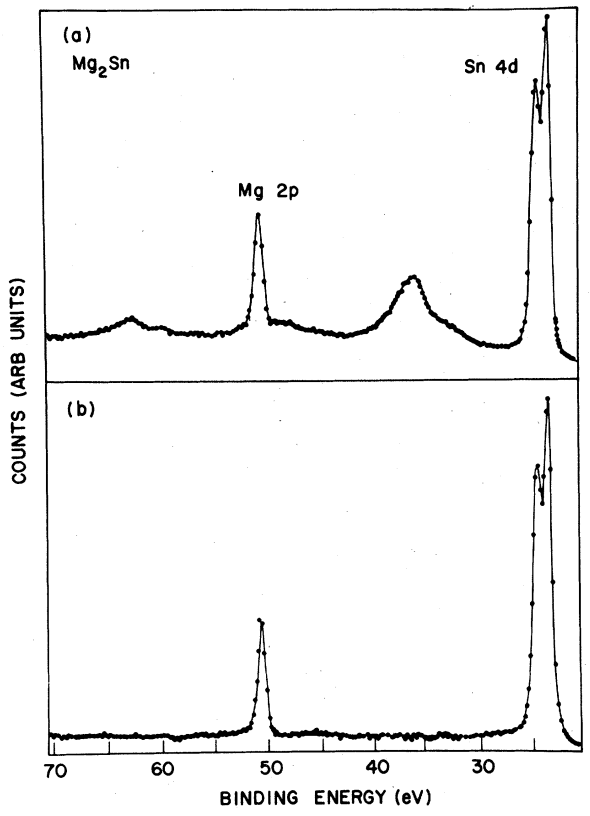

FIG. 3. Experimental photoemission spectrum before and after correction for the plasmon losses in the region of the Sn 4*d* and Mg 2*p* core lines in Mg_2Sn.

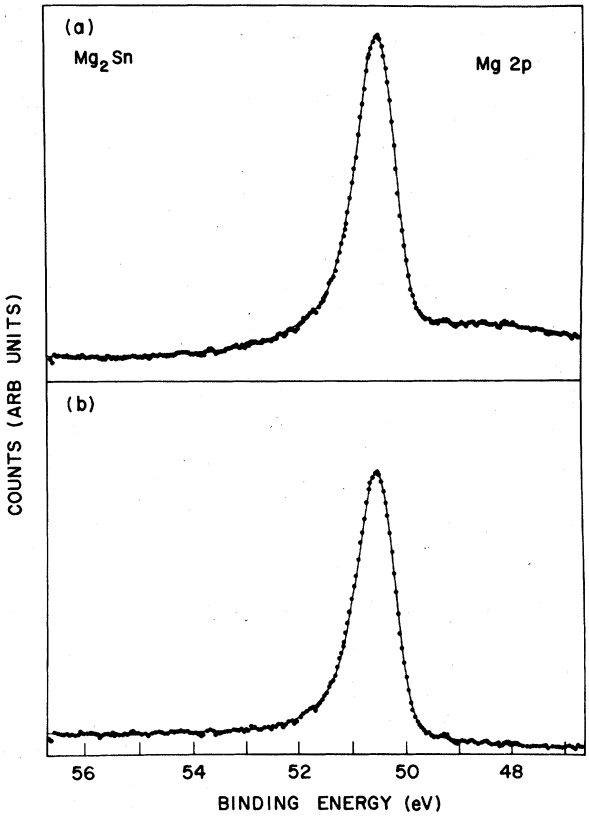

FIG. 4. Influence of the removal of plasmon contributions due to the Sn 4*d* lines on the line shape of the Mg 2*p* line in Mg_2Sn. (a) Experimental data, (b) after removal of plasmon losses.

to the weighted average of the measured plasmon energies of the pure constituents, while in the Au (and Pt) compounds the experimental plasmon energy is essentially equal to that of the group-III component. (The small differences which are observed can probably be attributed to changes in the valence-electron density due to volume changes.) The observations are in agreement with the calculated band structures which indicate free-electron behavior.

The experimental observations regarding the Mg_2X compounds are relevant to the band-structure calculations of Tejeda and Cardona[12] who treat the Mg_2X (X=Si, Ge, Sn) as purely ionic, in accord with the original concept of the Zintl phases. With the outer electrons of magnesium transferred to the X atom, the Mg s states would make a negligible contribution to the valence bands of the compounds. However, a comparison of the plasmon frequencies in the AuX_2 and the Mg_2X compounds with those of their constituents favors a covalent rather than a purely ionic model. This is in line with calculations of the charge-density distribution along the (111) direction in Mg_2Si by Bashenov *et al.*[21] which show that the valence electrons of Mg are incompletely transferred to the nearest neighbors and thus contribute significantly to the upper valence bands in Mg_2Si. Owing to the close similarity of the band structure this is expected to hold for the heavier Mg_2X compounds as well. The plasmon energies for Mg_2Sn and Mg_2Pb given in Table I are in excellent agreement with the free-electron values of 12.1 and 12.0 eV, respectively.

TABLE I. Bulk-plasmon energies ($\hbar\omega_b$) in the intermetallics and their constituent metals.

Compound AB_2	$\hbar\omega_b(A)$	$\hbar\omega_b(B)$	$\hbar\omega_b(AB_2)$
Mg_2Sn	14.3	10.6	12.0
Mg_2Pb	14.5	10.6	12.0
$AuAl_2$		15.7	15.1
$AuGa_2$		14.2	15.1
$PtGa_2$		14.2	15.5

MND EFFECT

The application of Eq. (4) to determine the many-body character of the line shape of XPS lines has been described in detail.[9] In the present work the instrumental resolution function, which had been determined independently, was folded into Eq. (4) and the resulting line shape fitted to the experimental data by adjusting α and γ. Figure 5 shows an example of a fit to experimental data corrected for the plasmon-loss contributions. The resulting singularity indices for the intermetallics and their constituent metals are given in Table II.

The trends in the singularity indices can be understood in terms of the Friedel phase shifts. In fcc Al with three electrons in the conduction band, α is 0.115. This is smaller than the minimum value of $\frac{1}{8}$ obtainable with s- and p-phase shifts alone, indicating that d-phase shifts are non-negligible. Recent analyses[22] have established a set of s-, p-, and d-phase shifts compatible with both the XPS and x-ray absorption edge data for Al. In bct (body-centered tetragonal) In, which also has three electrons per In atom in the conduction band, a quite similar value of α is obtained. The details of the lattice are clearly less important than the electron-to-atom ratio, provided the bands are free-electron-like. The simple cubic B sublattice of the AB_2 gold compounds is predominantly responsible for screening a core hole on a B atom. Except for the effects of charge transfer it also contains three electrons per B atom. The corresponding value of α for Ga and In in $AuGa_2$ and $AuIn_2$ are consequently close to those of the pure metals. The small singularity index in metallic Au reflects the strong deviation from free-electron behavior in the gold conduction band and the presence of appreciable $5d$ character at the Fermi energy.[23] In the AuX_2 compounds the Au $5d$ band narrows and drops well below E_F, greatly reducing the unoccupied $5d$ state density. The expected increase in the Au singularity index is experimentally verified.

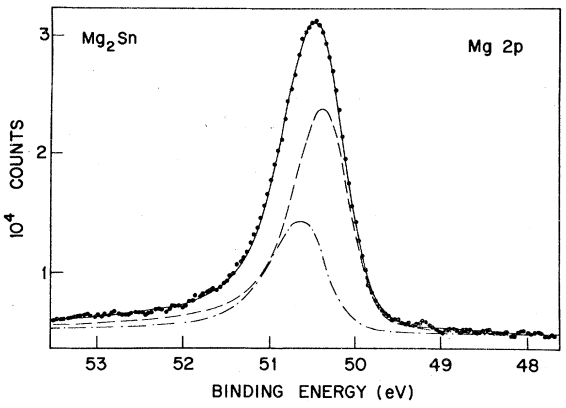

FIG. 5. Fit of the Mg $2p$ line in Mg_2Sn using Eq. (4) and the experimentally determined instrumental resolution function. The dashed lines show the $2p_{3/2}$ and $2p_{1/2}$ line separately. The intensity ratio was constrained to the theoretical value of 2.0.

TABLE II. Singularity indices (α) in the intermetallics and their constituent pure metals. The value of Ga metal is obtained by interpolation between Al and In metal. The uncertainty in α is generally ±0.01.

Compound AB_2	$\alpha(A)$ Pure metal	$\alpha(B)$ Pure metal	$\alpha(A)$ AB_2	$\alpha(B)$ AB_2
Mg_2Sn	0.12	0.13	0.04	0.09
Mg_2Pb	0.13	0.13	0.04	0.09
$AuGa_2$	0.04	(0.12)	0.08	0.115
$AuIn_2$	0.04	0.11	0.08	0.11

It was unexpectedly found that the core-electron spectra of Mg_2Sn and Mg_2Pb could also be fitted by the technique described, yielding the "pseudosingularity indices" shown in Table II. It must be realized, however, that the many-body line shape exemplified by Eq. (4) is realized only if the density of states is nonzero and at least approximately constant near E_F. These conditions are satisfied neither in a semiconductor such as Mg_2Sn nor in a semimetal such as Mg_2Pb. It has been previously pointed out, however, that band-gap excitations in a semiconductor can produce a loss tail which closely resembles the tail of the many-body line shape, especially when the band gap is much smaller than the instrumental resolution.[24] In the case of Mg_2Sn a small amount of metallic Sn was found in the analysis of the $3d$ and $4d$ lines. This suggests that the material may have been tin-rich, providing an alternate explanation for the metallic behavior. A third possibility is provided by the recent analysis of the C $1s$ line of graphite, a semimetal in which final-state excitonic effects were shown to be important.[25] The rather large singularity index found for Mg in both Mg_2Sn and Mg_2Pb could be indicative of a similar effect in these compounds. In essence it would require the formation of an excitonic state just above E_F when an Mg atom in these compounds is core ionized. The many-body response must then be calculated in the presence of this state. Further analysis here must await independent verification of the existence of this hypothetical excitonic state. It is important to recognize, however, that the fact that it is possible to fit data with the many-body line shape cannot be used to conclude that the material is a (simple) metal.

TABLE III. Charge transfer in CaF_2-structure compounds.

Compound AB_2	δE [a] (A) (eV)	δE [a] (B) (eV)	δz_a [b]
Mg_2Sn [c]	−0.60	0.75	−0.44
Mg_2Pb	0.34	1.55	−0.40
$AuAl_2$ [d]	2.05	0.95	−0.18
$AuGa_2$ [d]	1.33	0.51	−0.26
$AuIn_2$ [d]	1.13	0.40	−0.31

[a] Change in core-electron binding energy from the value in the pure metal, both measured from the Fermi level.

[b] Charge transfer to the A atom in units of $|e|$. The negative sign indicates that the A atom becomes negative.

[c] The following values were used for the work functions: Mg 3.6, Sn 4.4, Pb 4.0, Au 5.1, Al 4.25, Ga 4.0, In 3.8 eV.

[d] The relaxation term for the Au atom was taken as 1.2 eV. See Ref. 2.

CHARGE TRANSFER

In order to estimate the charge transfer the equations of Ref. 2 were generalized for an AB_2 compound, yielding

$$\delta z_a = \frac{e(\phi_b - \phi_a) + \delta E_a - \delta E_b + \delta R_a - \delta R_b}{F_a - M_a + F_b/2 - M_b/2} , \quad (6)$$

$$e\phi = e\phi_a - \delta E_a - \delta R_a + (F_a - M_a)\delta z_a . \quad (7)$$

The Coulomb integrals, F, were obtained by scaling the calculated value for Au $4f$ core levels by the atomic radius. The assumption here is that charge transfer involves the outer orbitals which also determine the atomic size. The Madelung potentials, M, were obtained using the approach of Ref. 26. The work functions are from the compilation of Fomenko[27] except where values for clean surfaces are available[28] (see Table III). The relaxation term δR, which represents the change in relaxation energy on alloy formation, will be important mainly in the case of Au which has empty d-band states in the pure metal but not in the compound. In the other metals there is no change in the character of the outer orbitals on alloy formation. Only the occupancy will change due to charge flow between atoms. In the present formulation there is then a cancellation of effects because loss of charge by one atom is accompanied by a gain of charge by the other. We have, therefore, ignored the relaxation term for the other metals. This is not the greatest source of uncertainty in this procedure, especially in view of the substantial cancellation between the poorly known Coulomb integrals and the Madelung potential. As a result the calculated charge transfers may be in error by as much as 50%.

The results of this analysis are summarized in Table III. The Sn and Pb in Mg_2X are found to gain 0.44 and 0.40 electrons, respectively. This is roughly 10% of the limiting value corresponding to filling of the $5p$ shell of Sn or the $6p$ shell of Pb. However, there is no reason to expect these compounds to approach the limiting ionic antifluorite state corresponding to $(Mg^{2+})_2Sn^{4-}$. Panke and Woelfel[29] have deduced a configuration for Mg in Mg_2Si corresponding to $Mg^{1.5+}$ from measurements of the electron-density distribution. However, they propose that the missing electrons are only incompletely transferred to the Si ion and contribute to the upper valence band in Mg_2Si. This agrees with the calculation of Bashenov *et al.*[21] Our result may also be compared with those of Levine[30] who obtained 0.224 for the ionicity of the bands in Mg_2Sn. Relative to the completely ionic state, this corresponds to a gain of 0.896 electrons by Sn in Mg_2Sn. For AuX_2 we find a transfer of electronic charge to the Au of 0.18, 0.26, and 0.31 in the Al, Ga, and In compounds. In every case the Fermi level in the alloy is calculated to lie close to that of the less electronegative constituent. It is gratifying that these crude estimates yield a consistent sign and a reasonable magnitude for the charge transfer. The sign of the charge transfer is such that all the compounds studied should be classified as antifluorite-structure materials. However, it would be unwise to attach quantitative significance to the magnitude, bearing in mind the estimated ±50% uncertainty.

ACKNOWLEDGMENT

One of the authors (P.v.A.) wants to thank the Netherlands America Commission for Educational Exchange for a Fulbright-Hays research scholarship.

*Present address: KFA-IFF, Postfach 1913, D-5170 Jülich, West Germany.

[1] See F. Laves and others, in *Intermetallic Compounds*, edited by J. H. Westbrook (Wiley, New York, 1967), p. 127ff.

[2] G. K. Wertheim, R. L. Cohen, G. Crecelius, K. W. West, and J. H. Wernick, Phys. Rev. B 20, 860 (1979).

[3] A. F. Wells, *Structural Inorganic Chemistry* (Clarendon, Oxford, 1962), p. 1013.

[4] B. I. Lundqvist, Phys. Konden. Mater. 9, 236 (1969).

[5]J. J. Chang and D. C. Langreth, Phys. Rev. B 5, 3512 (1972); *ibid.* 8, 4638 (1973).
[6]G. D. Mahan, Phys. Rev. 163, 612 (1967).
[7]P. Nozières and C. T. deDominicis, Phys. Rev. 178, 1097 (1969).
[8]S. Doniach and M. Šunjic, J. Phys. C 3, 285 (1970).
[9]P. H. Citrin, G. K. Wertheim, and Y. Baer, Phys. Rev. B 16, 4256 (1977).
[10]J. H. Wernick (unpublished).
[11]J. H. Scofield, J. Electron Spectrosc. 8, 129 (1976).
[12]J. Tejeda, M. Cardona, N. J. Shevchik, D. W. Langer, and E. Schönherr, Phys. Status Solidi B 58, 189 (1973); J. Tejeda and M. Cardona, Phys. Rev. B 14, 2559 (1976).
[13]M. Y. Au-Yang and M. L. Cohen, Phys. Rev. 178, 1358 (1969).
[14]J. P. Van Dyke and F. Herman, Phys. Rev. B 2, 1644 (1970).
[15]F. Vazquez, R. A. Forman, and M. Cardona, Phys. Rev. 176, 905 (1968).
[16]W. J. Scouler, Phys. Rev. 178, 1353 (1969).
[17]A. C. Switendick and A. Narath, Phys. Rev. Lett. 22, 1423 (1969).
[18]J. P. Jan, W. B. Pearson, M. Saito, M. Springford, and T. M. Templeton, Philos. Mag. 12, 1271 (1965).
[19]J. T. Longo, P. A. Schroeder, and D. Sellmyer, Phys. Lett. 25, 747 (1967).
[20]P. M. Th. M. van Attekum and J. M. Trooster, Phys. Rev. B 18, 3072 (1978).
[21]V. K. Bashenov, A. M. Mutal, and V. V. Timofeenko, Phys. Status Solidi B 87, K77 (1978).
[22]P. H. Citrin, G. K. Wertheim, and M. Schlüter, Solid State Commun. 32, 429 (1979).
[23]Y. Yafet and G. K. Wertheim, J. Phys. F 7, 357 (1977).
[24]G. K. Wertheim and D. N. E. Buchanan, Phys. Rev. B 16, 2613 (1977).
[25]P. M. Th. M. van Attekum and G. K. Wertheim, Phys. Rev. Lett. 43, 1896 (1979).
[26]G. C. Benson and F. van Zeggeren, J. Chem. Phys. 26, 1083 (1957).
[27]V. S. Fomenko, in *Handbook of Thermionic Properties*, edited by G. V. Samsonov (Plenum, New York, 1966).
[28]D. E. Eastman, Phys. Rev. B 2, 1 (1970).
[29]D. Panke and E. Woelfel, Z. Kristallogr. 129, 9 (1969).
[30]B. F. Levine, J. Chem. Phys. 59, 1463 (1973).